CPT Prediction of Liquefaction Resistance using the CPT Soil Characterization Curve Lookup Technique

Conference Paper · June 2018

CITATIONS
0

READS
81

1 author:

Richard Olsen
independent
53 PUBLICATIONS **399** CITATIONS

SEE PROFILE

CPT Prediction of Liquefaction Resistance using the CPT Soil Characterization Curve Lookup Technique

Richard S. Olsen, PhD PE[1]

[1]Senior Policy Advisor and Technical Lead for Geotechnical Engineering,
Engineering & Construction Division,, U.S. Army Corps of Engineers (USACE) Headquarters,
441 G Street NW, Washington DC 20314 e-mail: Richard.S.Olsen.civ@mail.mil

ABSTRACT

The author has published specialized techniques to interpret Cone Penetrometer Test (CPT) data for prediction of liquefaction for over 30 years, starting in 1984. These techniques have been updated numerous times, most recently in 2015. In all these cases, the technique generated contours of Liquefaction resistance ratio on the CPT soil characterization chart using field and laboratory data. The problem is that the shapes of these contours are always too difficult to represent by even the most complex of equations. The author has developed software to predict liquefaction resistance using this approach, and this technique has been verified by other researchers using point-to-point data comparisons. This update reflects important observations made in the last three years. The approach indirectly accounts for all soil types and relative strength consistencies without requiring the equivalent clean sand approach.

INTRODUCTION

Liquefaction Cyclic Resistance Ratio (CRR) is by definition liquefaction triggering resistance, namely liquefaction resistance (strength) divided by vertical effective stress. Normalized $CRR_{M=7.5,\sigma'=1atm,\alpha=0}$ is typically shown in other publications but for this paper will be shown as CRR_e (representing "equivalent" because a subscript of 1 or n would only represent 1 atm) and the earthquake-induced normalized Cyclic Shear Stress Ratio ($CSR_{M=7.5,\sigma'=1atm}$) will be shown as CSR_e. All equations and plots in this paper use normalized atmospheric pressure units (atm).

The basic approach in this paper for Cone Penetrometer Test (CPT) prediction of liquefaction resistance triggering is to use CRR_e surface contours (much like ground contours) on the CPT Soil Characterization Chart (Log-log plot of F_r versus Q_{T1}). This paper is a major update from Olsen (2015) and which was built on the sequence of improvements from Olsen (1997), Olsen & Koester (1995), Olsen (1988), and originating from Olsen (1984) shown in Figure 1. The first published comprehensive approach for CPT predicted of CRR_e of all soil types ranging from clean sands to clay was Olsen (1984), and at the time it was based on field observations of liquefaction, prediction of SPT (Douglas, Olsen, and Martin, 1981), and cyclic laboratory tests. The purpose of this paper was to improve the shape of the CRR_e contour surface from Olsen (2015) in Figure 1c. Changing the CRR_e contour surface is much like changing the shape of a protective cover sheet over a sofa by adding or removing blankets and pillows between the cover sheet and sofa.

For decades the conventional approach for CPT based prediction of liquefaction resistance was to initially convert the normalized cone resistance (Q_{T1}) to equivalent clean sand normalized cone resistance (q_{c1Ncs}) and then use it to predict CRR_e. The Boulanger & Idriss (2014) method is the de facto US standard. The equivalent clean sand concept originated with Standard Penetration Test (SPT) liquefaction prediction in the early 1980s by H. Bolton Seed because of issues with characterizing the SPT for sands with high fines content. The equivalent

Olsen, R.S., (2018) "CPT Prediction of Liquefaction Resistance using the CPT Soil Characterization Curve Lookup Technique,"
ASCE Geotechnical Earthquake Engineering & Soil Dynamics V conference, Austin TX – 2018

clean sand procedure is merely a means to simplify data evaluation; it will be shown in this paper to introduce inaccuracies because there really is no equivalent clean sand cone resistance.

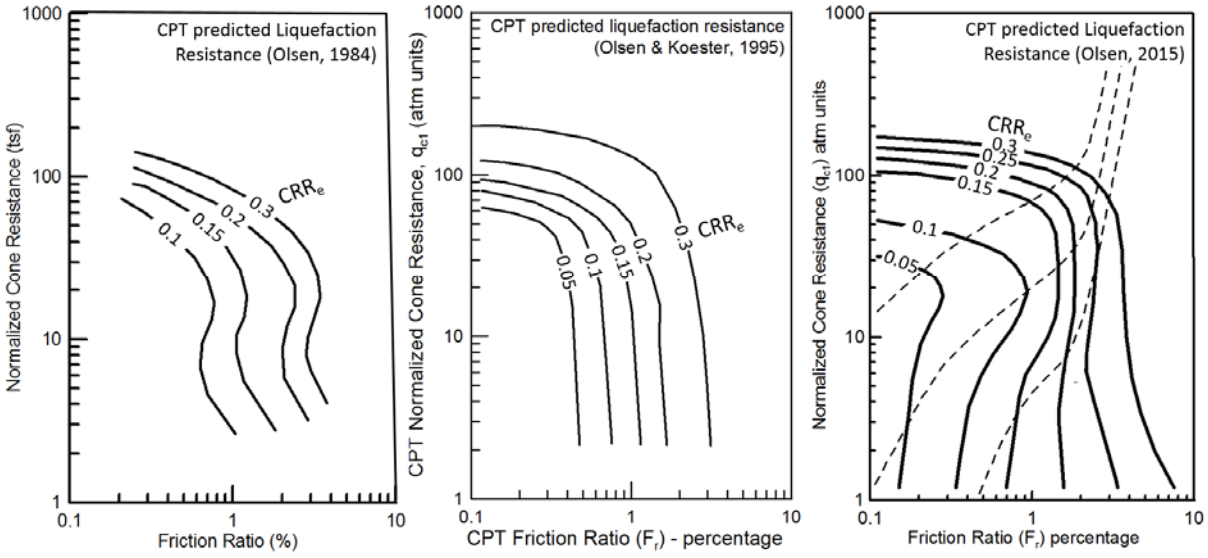

Figure 1. Historic approaches for chart based prediction of liquefaction resistance

Moss et al. (2006) presented historic research efforts for a probability of liquefaction P_L=15% for use as a conservative deterministic current practice (as reference P_L=50% represents 50% probability of liquefaction triggering with a corresponding Factor-of-Safety (FoS) of 1.0).

This paper used the well-established CPT liquefaction database most recently reported by Boulanger & Idriss (2014) which was an update from Moss et al. (2006). The Moss et al. (2006) database contains data with average ± one standard deviation range information whereas Boulanger & Idriss (2014) removed range information but added new data such as from the 2011 Christchurch earthquake.

PROCEDURE

Designing software for curve lookup. Developing software is required for predicting CRR_e based on CRR_e contour lines drawn on the CPT soil characterization chart. This section describes the basic of how to write the curve lookup procedure. The first step is to extend all predictive CRR_e contours beyond chart limits, shown as B-E lines in Figure 2a, ensuring that contour ends are beyond the adjacent chart contour intersections (C lines). The next step is to determine the curve lookup method: either XYC or YXC. The X in XYC implies that the search starts with the X axis, then uses the Y axis, and the final step is to calculate the C curve value. The R shaped curves in 2b cannot be used for the XYC procedure because for a given X values there are two contour intersections shown as T points. The V curves can be used with the XYC procedure. Each line in Figure 2c will be evaluated using the XYC procedure. For the given X value the Points E and F can be calculated for each contour line. The corresponding y values (i.e. yC1, yC2, yC3, etc) for each S point are calculated using linear calculations based on points E and F and given X. S points locations are determined until two of them bound the given Y, in this case yC2 and yC3. The curve value Cp is calculated using linear interpolation based on the

given Y, points yC2 and yC3, and curves values C2 and C3.

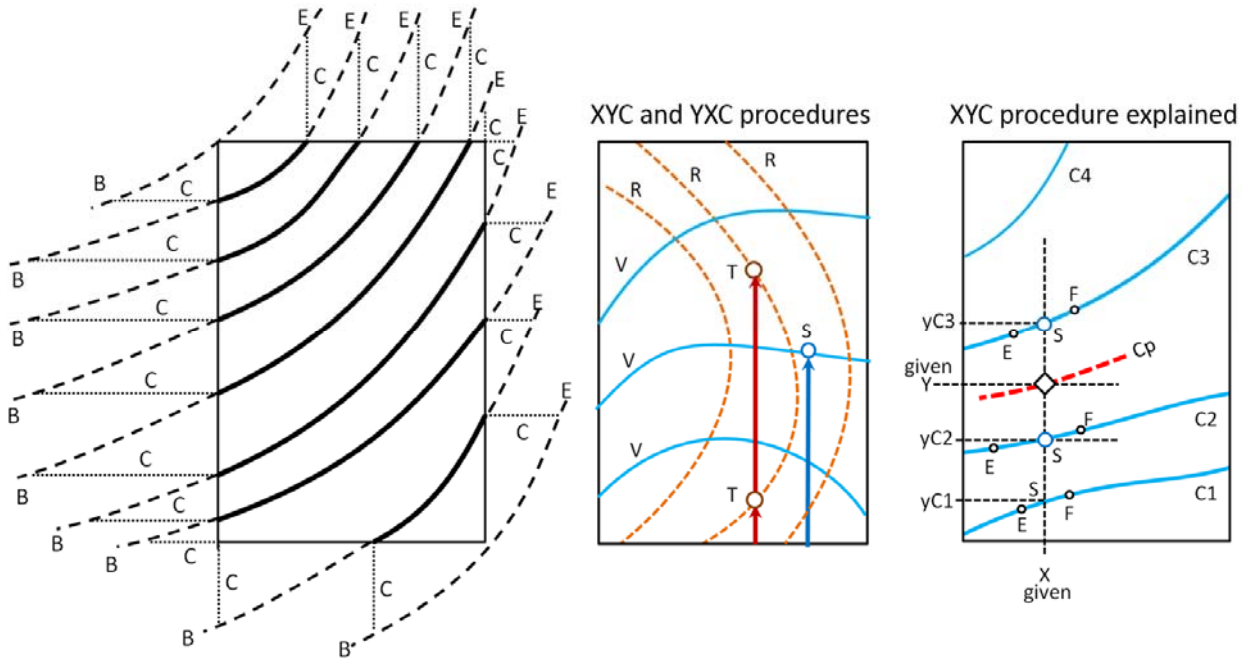

Figure 2. Curve Lookup software steps, a) Setup, b) Method selection, c) Procedure

Outlier Definition. The group of CRR_e contour lines in each of the Figure 1 charts represent a 3D CPT predictive CRR_e contour surface as illustrated in Figure 3. Each CPT database point value of Q_{T1}, F_r, and CSR_e together with the corresponding working database ranges can be visually shown by one of the boxes in Figure 3. If the database CSR_e value is below the CRR_e surface, then the calculated predicted liquefaction Factor of Safety (FoS) is greater than 1. Outliers are defined as either

1) Unconservative Outlier (UO) when liquefaction is not predicted (FoS>1) to occur but field liquefaction was observed as illustrated by the red box designated as U, or

2) Conservative Outliers (CO) when liquefaction is predicted (FoS<1) to occur but field liquefaction was not observed, as the blue box designated as C.

While CO and UO data can be used to improve the CPT predictive CRRe surface location, the Anticipated Behavior (AB) data (A boxes in figure 3) matches the criteria and therefore cannot be used.

General procedure. There are three steps to find the optimized CRR_e contour surface;

1) Iteratively move and reshape CRR_e "test" contour surface to decrease the number of and magnitude of UO and CO,

2) Calculate "quality of fit" cross correlation for UO and CO data,

3) Fine tuning the CRR_e contour surface to achieve the correct probability of prediction.

Step 1) Observational procedure. Iteratively reshaping CRR_e "test" contour surface requires a criteria to shows that each successive change is improving the quality of fix to the CRR_e database values. The procedure is to graphically show the direction and magnitude of conservative and unconservative outliers for each "test" CRR_e contour surface improvement.

A CRR_e contour surface is defined with a data computer file containing several CRR_e lines (generally CRR_e of 0.05 to 0.3). The procedure is
1) Make a CRR_e contour surface "test" data file having individual CRR_e lines,
2) Calculate which CSR_e database values are unconservative or conservative outliers,
3) Have a means to plot the unconservative and conservative outliers as vectors on the CPT soil characterization chart, and finally
4) Examine the plotted outlier vectors for the purpose of creating an improved contour surface shape,
5) Repeat.
This process requires a new computer data file for each iteration.

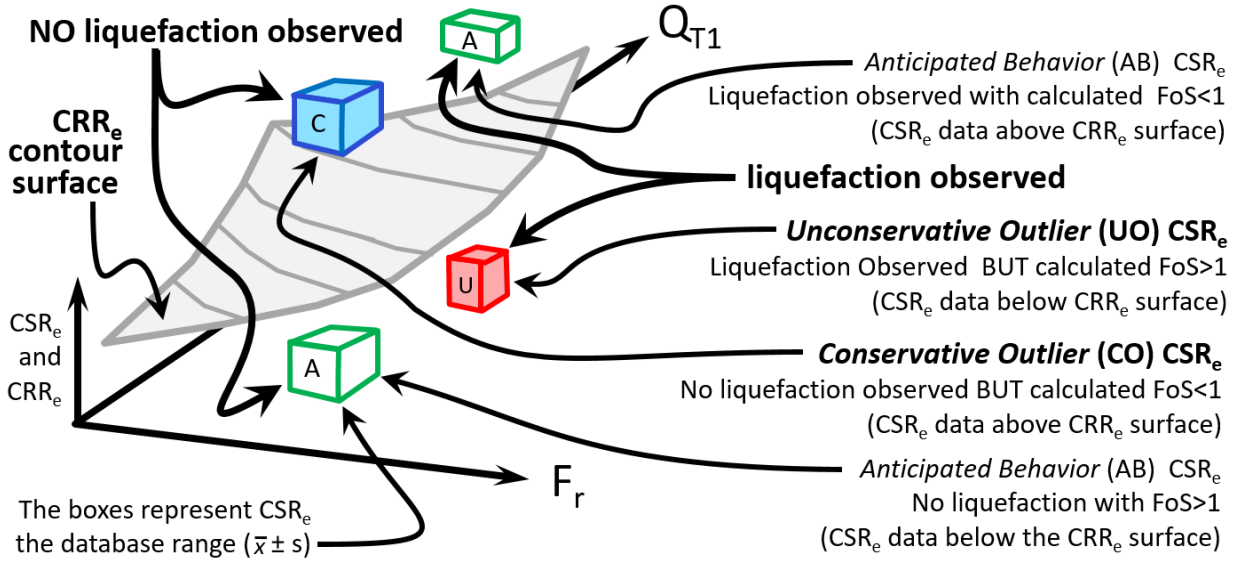

Figure 3. Definition of the CRR_e contour surface and CSR_e data Outliers

Figure 4 illustrates the CPT soil characterization chart (Log_{10} F_r versus Log_{10} Q_{T1}) with CRR_e and CSR_e on the vertical axis. Soil type lines can be conceptually plotted as shown on the Fr versus Q_{T1} plane (in blue). An UO CSR_e data value is shown in Figure 4 (the red box at Box E showing average and range) and is under the CRR_e contour surface with FoS<1. The corresponding predicted CRR_e value (Point D) on the "test" CRR_e predictive contour surface is also shown. The predicted CRR_e and database CSR_e points are on the same vertical Z line which means that both CRR_e and CSR_e have the same Q_{T1} and F_r values on the CPT Soil Characterization chart. The CSR_e (point E) and predictive CRR_e (point D) when plotted on the CPT soil characterization chart are at the same location. While you can see this difference in a 3D chart (Figure 4) you cannot see the difference on the 2D CPT soil characterization chart. A special graphical procedure was required to see the CSR_e and CRR_e combinations on the CPT soil characterization chart. The idea is to find the closest point on the CRR_e contour surface to the CSR_e database point in the Log_{10}-Log_{10} space. In Figure 4 the closest CRR_e point (on the contour surface) to the CSR_e point (E) is point G. This procedure required special routine inside the software already described in this paper. Point G and E can be projected down to CPT soil characterization chart shown as points H and F. CRR_e and CSR_e points can now be seen on the 2D CPT soil characterization chart.

The "Push" method. In Figure 4, if point G (i.e. closest CRR_e value on CRR_e contour surface) can be PUSH*ed* (together with the CRR_e surface) to point E then this Unconservative Outlier will change to Anticipated Behavior. This "Push" method is illustrated in Figure 5 showing how the CRR_e contour surface is locally pushed down and over to CSR_e point – much like pushing down on a blanket cover on top of a bed at specific location. The procedure is to calculate all database outliers and plot vector locations as illustrated by the red H to F arrow in Figure 4. Both charts in Figure 6 shows unconservative outliers as red and conservative outliers plot as blue – The vector thickness relates to the database quality value (thick lines for high quality data). Figure 6a shows the "Push" outlier vectors using the Olsen (1988) CPT predicted CRR_e contour surface – the number and magnitudes of outliers is large and most are unconservative. After 24 iterations the results are shown in Figure 6b (from Olsen, 2015) having more CO vectors compared to UO vectors.

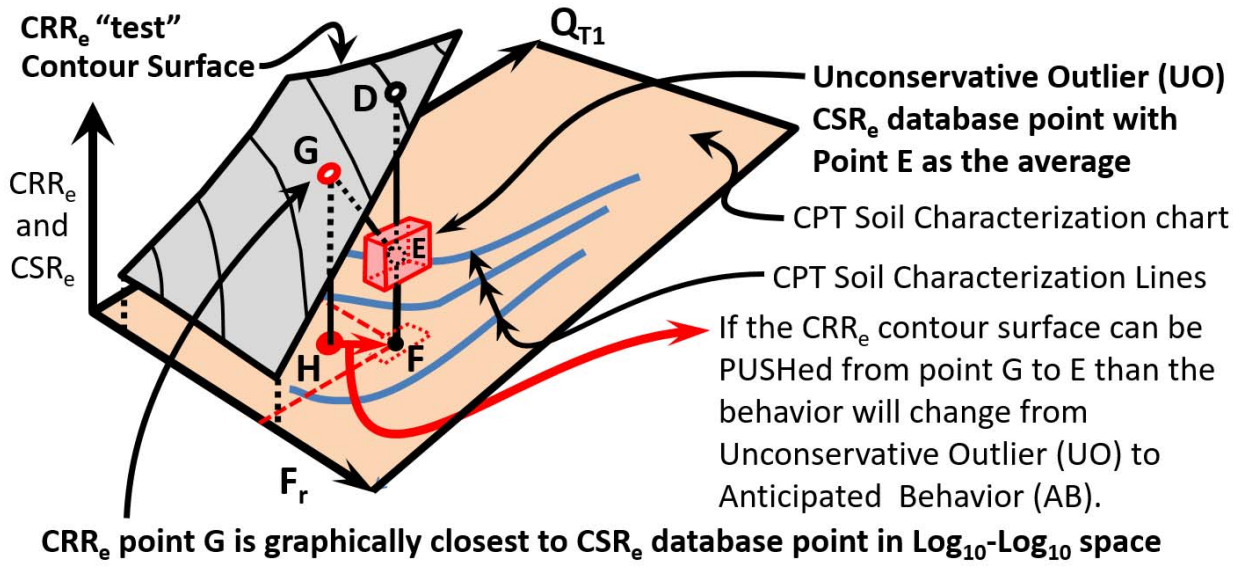

Figure 4. Defining the CRR_e contour surface and differentiating CRR_e and CSR_e

Step 2) Quality of fit Cross correlation procedure. The second step is to provide a quality of fix calculation using a cross correlation equation shown in Equations 1 – lower values reflect better fit. This equation provides a means to show that each graphic iteration is improving the quality of fit. All Unconservative Outlier vectors are used to determine A_u and likewise all Conservative Outlier vectors are used to determine A_c.

$$A_u \text{ and } A_c = \frac{\Sigma\left(\frac{|CRR_e - CSR_e|}{CRR_e} Q_f \right)}{N_{db}} \qquad (1)$$

with

CRR_e = CPT predicted Liquefaction Resistance (Point D on contour surface in Figure 4)
CSR_e = CSR_e from database (point E in Figure 4).
Q_f = Quality index (from 0.6 to 1.0) for each database point reflecting C, B, or A quality
N_{db} = Total number of items in database

Step 3) Optimize CRR_e surface to P_L=15%. The third step is to modify the selected CRR_e contour surface to represent 15% probability of liquefaction prediction, P_L=15% (Moss et al. 2006). The procedure is to rise and lower the CRR_e contour surface in 0.0025 increments (illustrated on the right side of Figure 7) while calculating A_c and A_u. Plotting lines of A_c, A_u, and A_c+A_u versus ΔCRR_e (and the 15% designation) are shown on the left side of Figure 7. The final CRR_e contour surface position is locked at ΔCRR_e=0 when Unconservative Outlier A_u is 15% of A_u+A_c. This 15% represents the required 15% probability of prediction. The 15% to 50% probability difference of 0.022, i.e. $(\Delta CRR_e)_{15\text{-}50}$ in Figure 7, is within range of 0.02 to 0.04 reported from Boulanger & Idriss (2014) and lower than 0.03 to 0.04 from Moss et al. (2006).

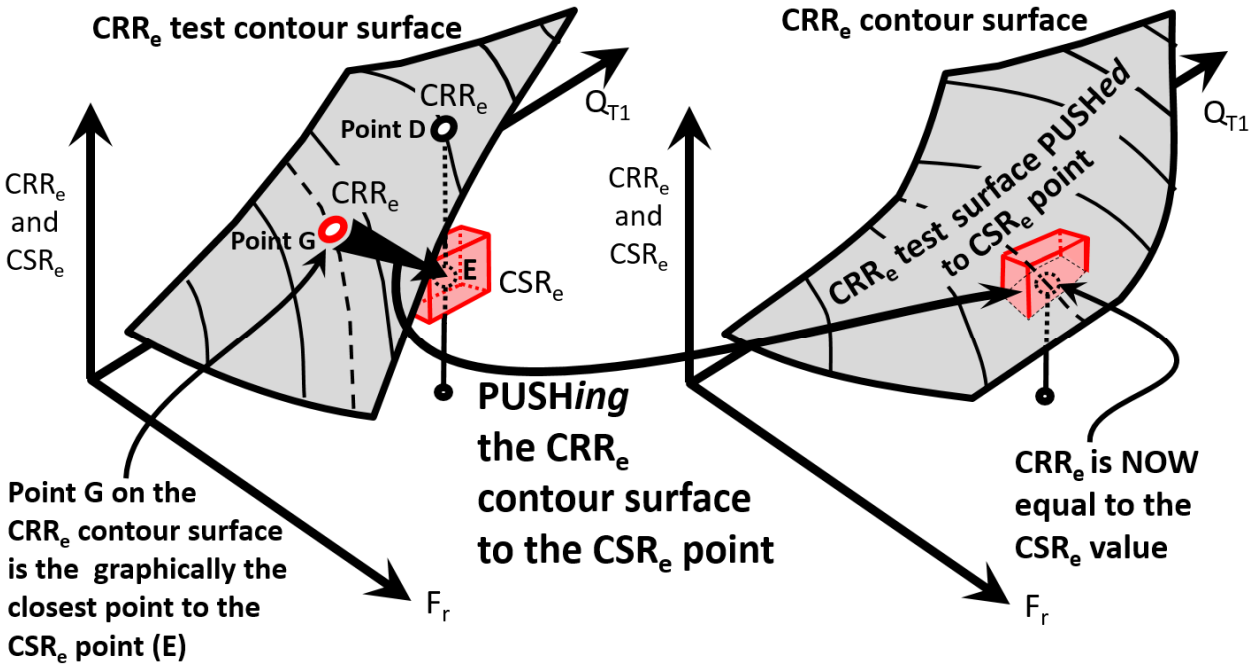

Figure 5. PUSHing the CRR_e contour surface to CSR_e database point.

RESULTS AND DISCUSSION

The final CRR_e contour surface in Figure 8 meets the standard for prediction of liquefaction resistance with a probability of P_L=15%. This chart is a major update based on three years of careful examination after Olsen (2015). The chart on the right is in linear scale to better show the location of CRR_e contour lines for sandy soils.

Converting equation-based methods to CRR_e contours. Equation-based methods (i.e. Boulanger & Idriss (2014), and Moss et al. (2006)) were converted to CRR_e contour surfaces using an iterative routine within the software developed in 2015 (Olsen, 2015) and modified during this update. This step allows equation-based methods (e.g. Boulanger & Idriss (2014)) to be compared to chart based methods (i.e. Olsen (1964, 1995, 1997, and 2015) and the results from this paper).

The procedure is to initially subdivide the CPT soil characterization chart into 60,000

boxes by dividing the $\log_{10} Q_{T1}$ axis into 300 vertical positions versus the $\log_{10} F_r$ axis into 200 horizontal positions. The software starts by stepping through each CRR_e contour line (i.e. CRR_e = 0.05, 0.1, 0.15, 0.20, 0.25, & 0.30). For each CRR_e contour line, the software calculates the equation-based CRR_e at each of these 60,000 boxes. If the calculated equation-based CRR_e meets a closure range criterion of 1% then the F_r and Q_{T1} point is saved for that CRR_e line contour. For example, the CRR_e=0.1 contour line (with a 1% closure criterion) has a CRR_e closure range of 0.099 to 0.101. After searching is completed for each CRR_e contour line, all the stored points are plotted, as a scatter plot, on the CPT soil characterization chart. The final step is to draw a CRR_e contour line through the narrowly focused cloud of plotted points. This step is repeated for each CRR_e contour line.

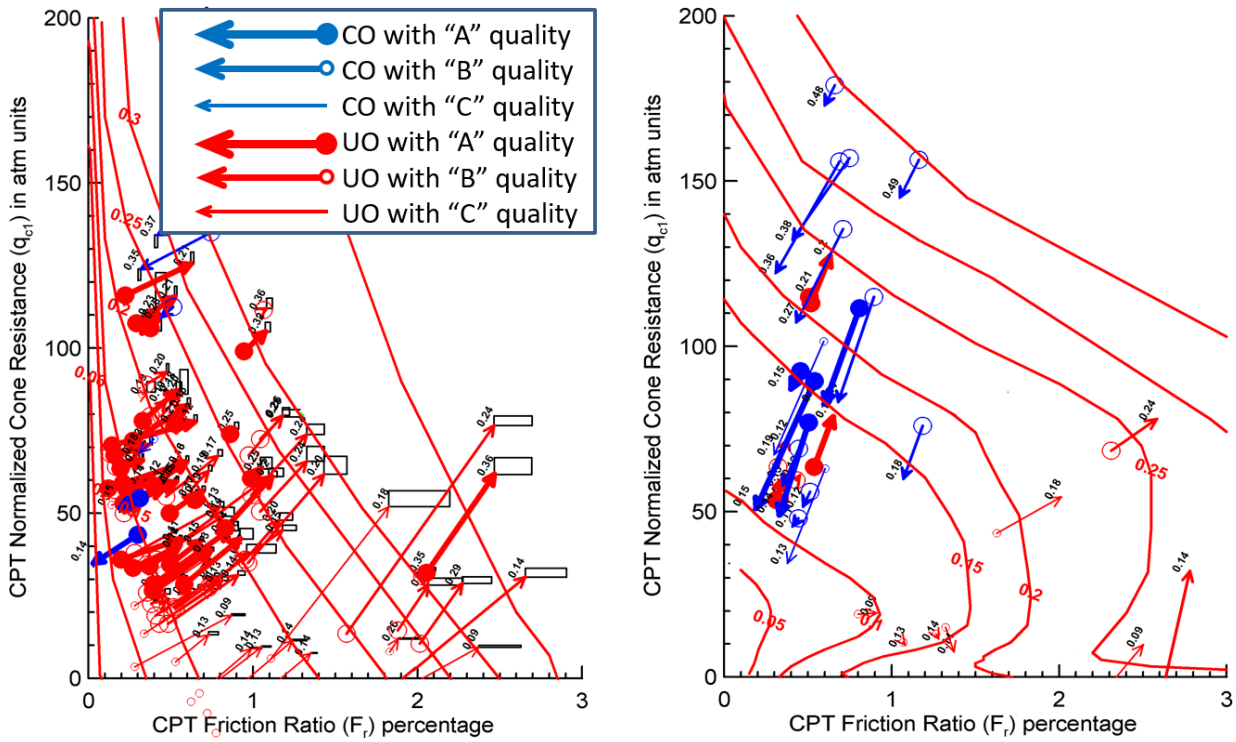

Figure 6. Computer output of outlier "PUSH" results, a) Olsen (1988), b) Olsen (2015)

Comparison of predictive methods. The final step is comparison of equation-based and chart-based CRRe methods in Figure 9a and 9b. While these figure are complicated there are several key observations that will be explained for each soil type.

Figure 9a shows selected CRR_e contour lines (using the software procedure from the previous section) for Boulanger & Idriss (2014) and Moss et al. (2006) together with a few contour lines from Olsen (1984, 1995, and 2015) and results from this paper. The abbreviations are B&I for Boulanger & Idriss (2014), M&S for Moss, Seed, Kayen, Stewart, Kiureghian, & Cetin (2006), and years are for Olsen (1984, 1995, 2015, and 2018 for this paper).

Sand Behavior. In Figure 9a and 9b, the Boulanger & Idriss (2014) method for CRR_e=0.11 to 0.3 shows a curious downward bend as well as an interesting behavior for CRR_e=0.1 (specifically at point W and line V). Boulanger & Idriss (2014) method shows for constant

CRR_e contour of from 0.11 to 0.3 at low F_r (see note B) in Figure 9b that Q_{T1} is at a constant level over a wide range of F_r even though the normalized sleeve resistance (f_{s1}) is increasing. It is not realistic for a given CRR_e level (in clean sand zone of the chart) to have a constant Q_{T1} level while the normalized sleeve resistance (f_{s1}) increases. It is more realistic for a given sand CRR_e constant level to have a balance of Q_{T1} decreasing with increasing F_r as also shown in Figure 9b (as note R).

CRR_e contours within the clean sand area at low F_r (of 0.1 to 0.6%) in Figure 9 for this paper were reshaped from Olsen (2105) (by only a few line thicknesses) such that CRR_e contours have a decreasing Q_{T1} as F_r increases. The CRR_e contours were also modified within the dirty sand to silt area to better reflect over consolidation of silts and sands. The lowest CRR_e contours from Olsen (2014) was reshaped based on review of the CPT database.

The CRR_e contour lines of 0.1 and 0.2 for all methods (i.e. this paper, Olsen (1984, 1995, 2015), Boulanger & Idriss (2014) and Moss et al. (2006)) intersect at two locations (Point A for CRR_e=0.15 and Point S for CRR_e=0.2) likely because all use the same data. Both of these points have CPT characterization chart classification of a high silt content sand (I_c = 2.05). Point W for CRR_e=0.1 is another location with equal contour value for this paper and other historic methods.

There are two long zones where Boulanger & Idriss (2014) CRR_e contours approximately match the contours from this paper, shown with blue hash symbol in Figure 9b. The red CRR_e contour lines from this paper for sands in Figure 9b show a gentle slope between these two hash areas. Boulanger & Idriss (2014) show a very non-linear behavior between these hash areas. The predicted CRR_e for this paper (with the gentle slope between the two hash areas) is higher than for Boulanger & Idriss (2014). The likely reason for this difference is that the intermediate calculation of the equivalent clean sand cone resistance (q_{c1Ncs}) for Boulanger & Idriss (2014) method introduces conservation.

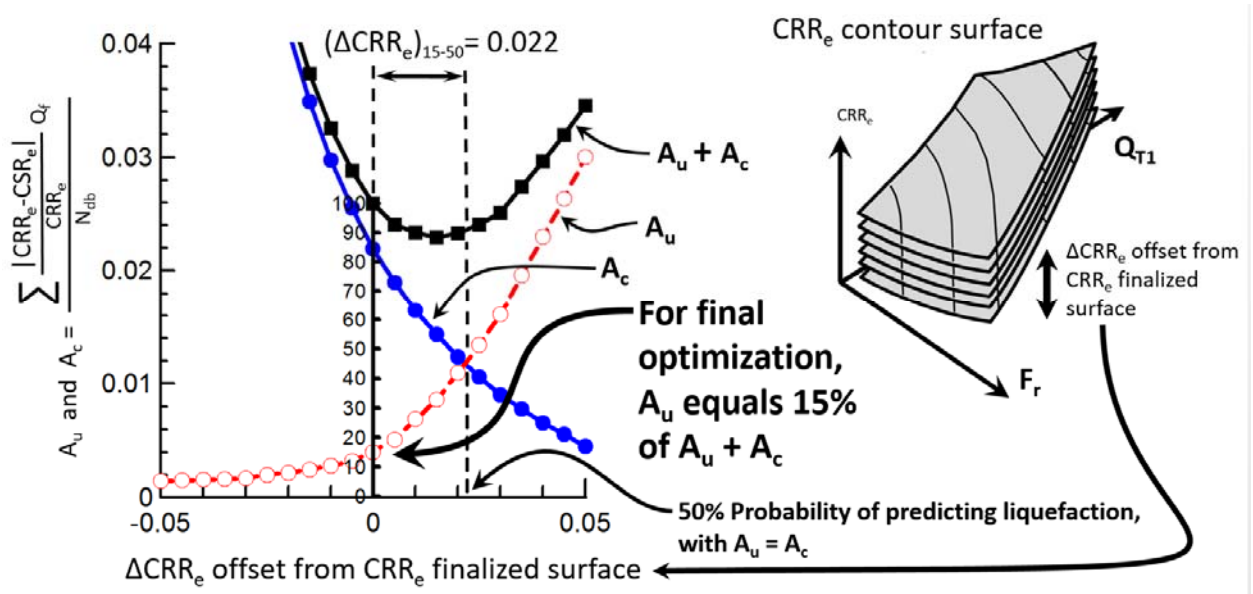

Figure 7. Optimizing cross correlation to determine liquefaction P_L=15%

Silt behavior. Typical normally consolidate non-sensitive silts are generally found within the "Silts" zone shown in Figure 9b and based on information from CPT database having a CRR_e

range of 0.12 to 0.21, laboratory values of CRR_e of 0.17 to 0.22 from Romero (1995) and Boulanger & Idriss (2004), and CRR_e of 0.15 to 0.22 from the author's records. Within the "Silts" zone the Boulanger & Idriss (2014) method is showing CRR_e contours from 0.11 to 0.14 (which is too low), whereas Olsen (2015) shows intersecting contours of 0.12 to 0.23. The CRR_e contours, for this updated paper, within this "Silts" zone are now 0.13 to 0.20, which better reflects data from the CPT database and cyclic laboratory data.

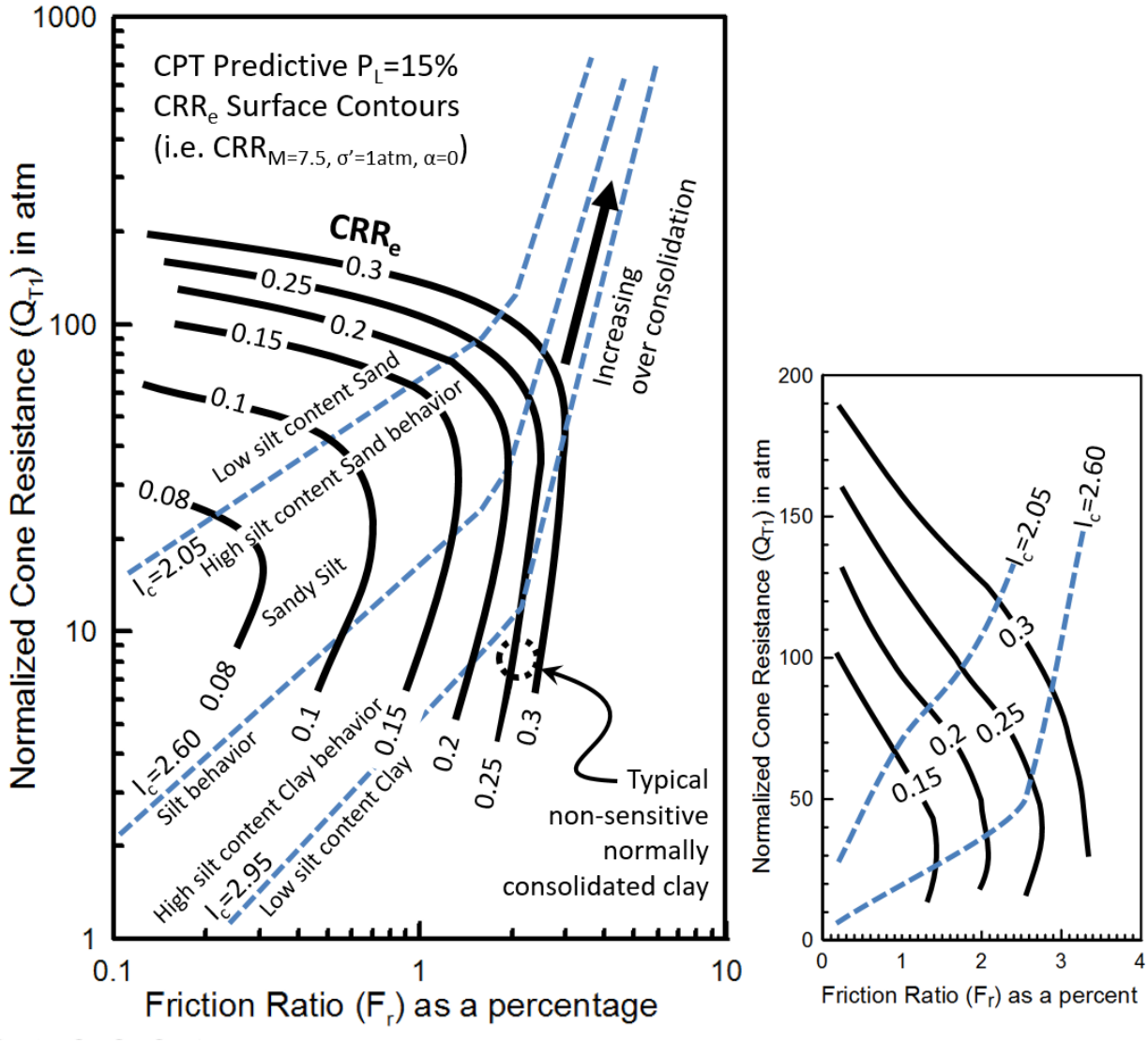

Figure 8. a) Final CPT predictive CRR_e contour surface, b) linear for sands

Clay behavior. Non-sensitive, low silt content, normally consolidated clay is typically plotted at the location shown in Figures 9a. Historic research infers that a strain based liquefaction criteria should have CRR_e equal to about 80% of clay static strength. A typical static normally consolidated undrained strength divided by vertical effective (i.e. $(c/p)_{NC}$) is approximately 0.31 which therefore would correspond to $CRR_e \approx 0.25$.

The Boulanger & Idriss method calculates a CRR_e=0.10 for typical normally consolidated clay but the method does specifically limit predictions to sandy silts to sands, i.e. I_c less than 2.65 (silt behavior) shown as solid blue lines in Figure 9b. The observation is that Boulanger & Idriss technique predicts an unrealistic low CRR_e for high silt content sand and this prediction of low CRR_e continues as the soil type transitions from silts to clay.

Over consolidation trends for clays are also shown Figure 9a. The CRR_e contour of 0.25 and 0.3 contours were reshaped for this paper to ensure CRR_e increases with increasing clay over consolidation. CRR_e trends were also terminated (in Figure 8) at low Q_{T1} where there is no supporting data.

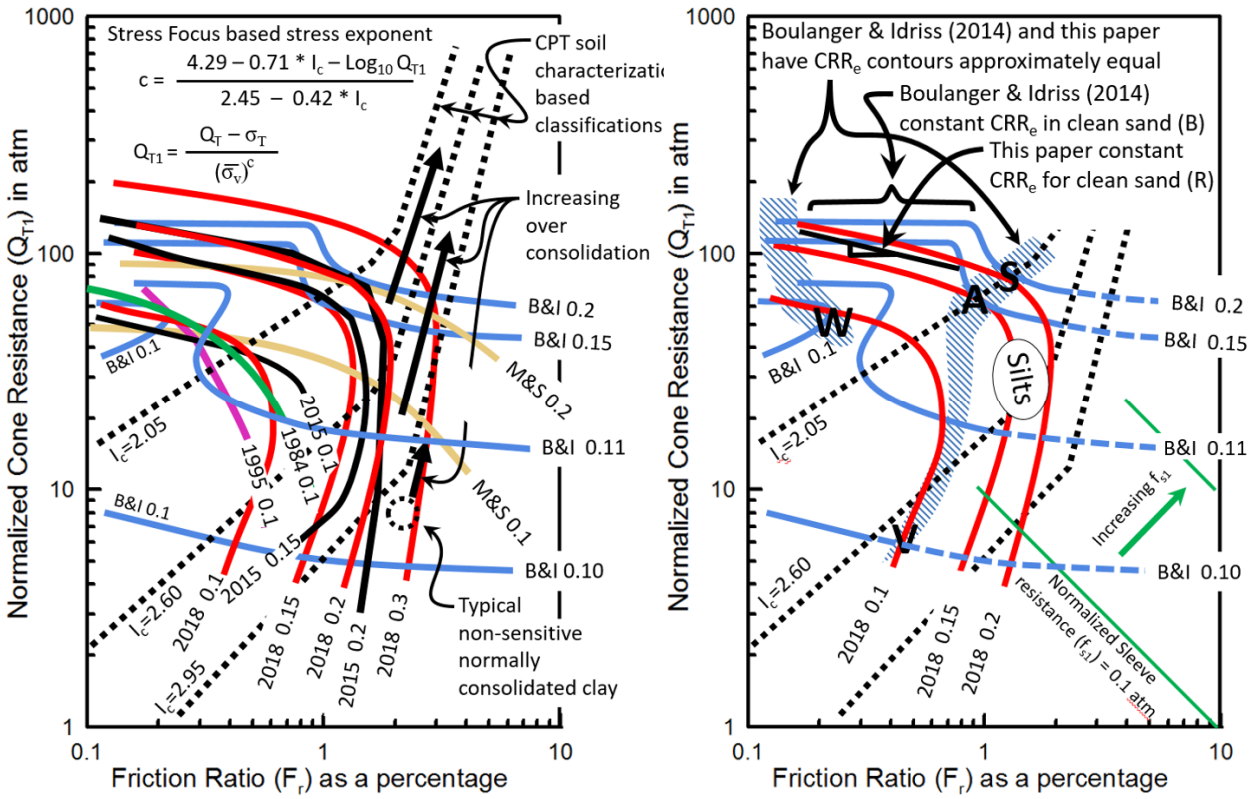

Figure 9. Comparison to historic CRR_e predictive methods a) All information, b) Detailed

EXAMPLE

An example is shown in Figure 10 from the Gainsborough Reserve, Christchurch, New Zealand, specifically sounding CPT_36417 from the New Zealand Geotechnical Database (www.NZGD.org.nz). This site has numerous layers of silty sand and silt which did not generate liquefaction boils on the ground surface during the 2010 September 4 or 2011 February 22 earthquakes.

The first chart on the left is a depth plot of CPT predicted soil type (I_c) with Unified Soil Classification System (USCS) symbols also shown. Plotting the CPT I_c on top of USCS symbols makes it easier for geotechnical engineers to visualize soil column character.

The middle chart is a depth plot of predicted CRR_e using the technique from this paper and from Boulanger & Idriss (2014). The Boulanger & Idriss (2014) method specifically only includes sandy soils (i.e. I_c<2.65) which is why only the sandy soil layers are plotted. The technique in this paper is for all soil types and in all cases the clay for this example has a predicted CRR_e > 0.23. Layering transitions and interbedding between clays and sands cause phantom layers and issues with predicted soil properties. Most of CRR_e jumping from 0.16 to 0.23 in this example are due to these layer transitional issues.

The chart on the right is the CPT soil characterization chart with contours of CPT predicted soil type I_c and CRR_e. The CRR_e are specifically only for CRRe = 0.1, 0.15, and 0.2 – red is for the CRR_e prediction from this paper and blue is for Boulanger & Idriss (2014). The green lines are CPT predicted soil type.

This example shows two depth zones from the left chart projected onto the CPT soil characterization chart on the right. Note how the sand example is plotting in the CPT soil characterization within the wide band of CRR_e=0.11 to 0.15 for the Boulanger & Idriss (2014) method and the band is shown with yellow shading – this wide range covers a major portion of all normally consolidated weak to typical silts and loose to medium dense sands. This band for CRR_e=0.11 to 0.15 is also why most of the plotted data in the middle chart for Boulanger & Idriss (2014) method is predicting CRR_e=0.115 to 0.13. The predicted CRR_e for the clay example using the technique in this paper is showing a CRR_e between 0.22 and 0.24, which is within the expected range for normally consolidated clay.

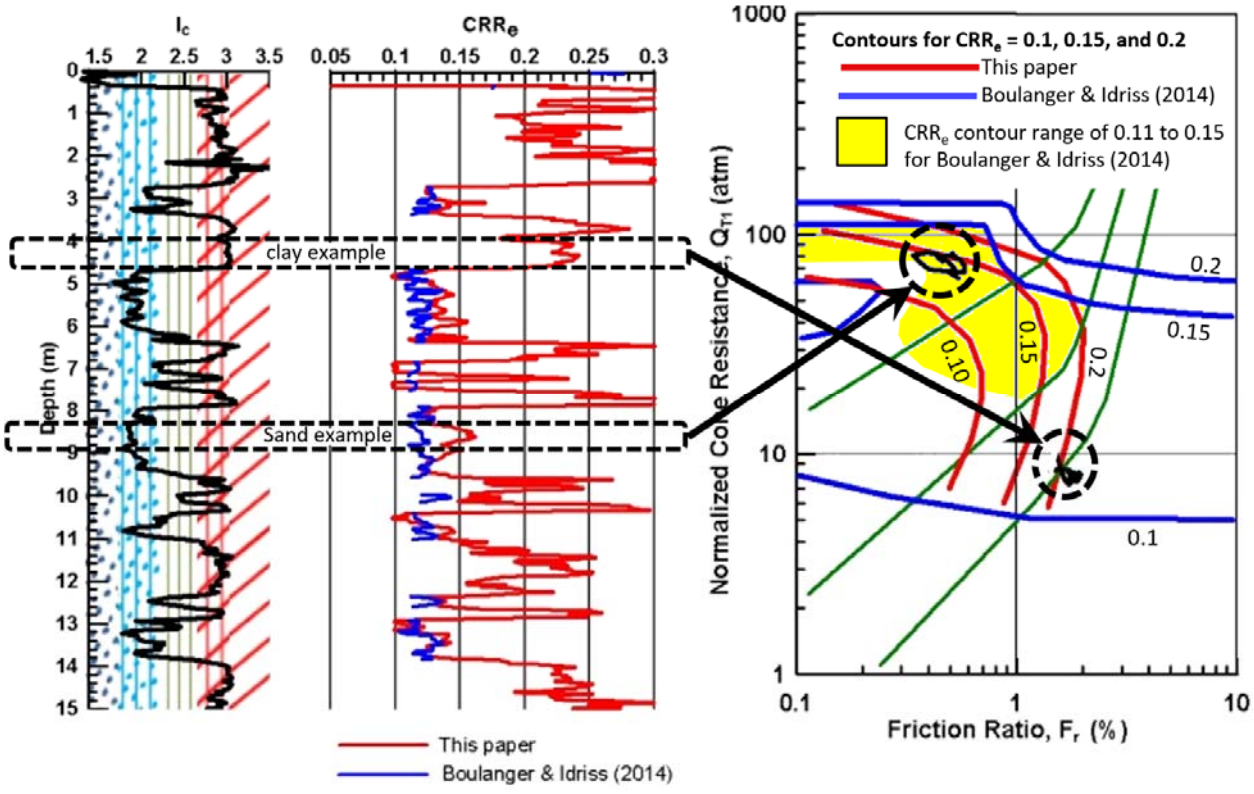

Figure 10. Comparison of techniques, Christchurch, New Zealand, for CPT_36415

Olsen, R.S., (2018) "CPT Prediction of Liquefaction Resistance using the CPT Soil Characterization Curve Lookup Technique,"
ASCE Geotechnical Earthquake Engineering & Soil Dynamics V conference, Austin TX – 2018

CONCLUSIONS

This paper for CPT-based prediction of liquefaction for sands to clay was a major update from Olsen (2015) after careful examination and critical review. The basic procedure was a graphic observation method, followed by an equation-based cross correlation calculation, and finally an optimization approach to achieve the 15% probability of occurrence. The final predictive CRR_e contour surface from this paper was compared to existing equation-based procedures that use the equivalent clean sand approach.

ACKNOWLEDGMENTS

This paper does not reflect recommendations, endorsement, or policy of the U.S. Army Corps of Engineers. I wish to also thank Dr. Joseph P. Koester for review of this paper.

REFERENCES

Boulanger, R.W., Idriss, I.M (2004). "Evaluating the Potential for Liquefaction or Cyclic Failure of Silts and Clays." UC Davis Ctr. for Geotech. Modeling, Report No UCD/CGM-04/01.

Boulanger, R.W., Idriss, I.M (2014). "CPT and SPT based Liquefaction Triggering Procedures." UC Davis Center for Geotechnical modeling, Report No UCD/CGM-14/01.

Douglas, Olsen, and Martin (1981). "Evaluation of the Cone Penetrometer Test for SPT-Liquefaction Assessment", In Situ Liquefaction Susceptibility, ASCE convention.

Moss, R. E. S., Seed, R. B., Kayen, R. E., Stewart, J. P., Kiureghian, and Cetin (2006). "CPT-Based Probabilistic and Deterministic Assessment of In Situ Seismic Soil Liquefaction Potential" J. of Geotechnical & Geoenvironmental Engineering, ASCE, Aug 2006.

Olsen, R. S. (1984). "Liquefaction analysis using the cone penetrometer test." Proc., 8th World Conf. on Earthquake Engineering EERI, San Francisco.

Olsen, R. S., and Koester, J. P. (1995). "Prediction of liquefaction resistance using the CPT." Proc., International Symposium on Cone Penetration Testing, CPT 95, Sweden.

Olsen, R. S. (1997). "Cyclic liquefaction based on the cone penetrometer test." NCEER Workshop on Evaluation of Soil Liquefaction, NCEE, Report No. NCEER-97-0022.

Olsen, R. S. (2015). "Prediction of Liquefaction Resistance using a Combination of CPT Cone and Sleeve Resistances – it's really a contour surface." 6th Intern. Conf. on Earthquake Geotech. Engineering, Christchurch, New Zealand.

Romero, S. (1995). The behavior of silt as clay content is increased. MS thesis, University of California at Davis.